

BRNO UNIVERSITY OF TECHNOLOGY
Faculty of Mechanical Engineering
Institute of Machine and Industrial Design

Ing. Daniel Kvarda

**EXPERIMENTAL INVESTIGATION
AND NUMERICAL MODELLING OF
TOP OF RAIL PRODUCTS**

**EXPERIMENTÁLNÍ VÝZKUM A NUMERICKÉ
MODELOVÁNÍ MAZIV PRO KONTAKT KOLA A
KOLEJNICE**

Shortened version of PhD Thesis

Branch: Design and Process Engineering

Supervisor: prof. Ing. Martin Hartl, Ph.D.

Keywords:

Wheel-rail contact, Friction management, Top of rail products, Numerical model, Tribology

Klíčová slova:

Kontakt kolo-kolejnice, Řízení tření, Maziva pro kolejový svršek, Numerický model, Tribologie

Místo uložení práce:

Oddělení pro vědu a výzkum FSI VUT v Brně.

CONTENTS

| | | |
|-------|---|----|
| 1 | INTRODUCTION | 4 |
| 2 | STATE OF THE ART | 5 |
| 2.1 | Top of rail products | 7 |
| 3 | SUMMARY AND CONCLUSION OF STATE OF THE ART | 12 |
| 4 | AIM OF THESIS | 13 |
| 4.1 | Scientific question and hypotheses | 13 |
| 4.2 | Thesis layout | 14 |
| 5 | MATERIALS AND METHODS | 15 |
| 5.1 | Laboratory measurements | 15 |
| 5.1.1 | <i>Optical ball on disc tribometer</i> | 15 |
| 5.1.2 | <i>Mini traction machine ball on disc tribometer</i> | 15 |
| 5.1.3 | <i>Torsion rheometer</i> | 15 |
| 5.2 | Numerical model | 16 |
| 5.3 | Test samples, experimental conditions and experiment design | 19 |
| 5.3.1 | <i>Paper A</i> | 19 |
| 5.3.2 | <i>Paper B</i> | 20 |
| 5.3.3 | <i>Paper C</i> | 22 |
| 6 | RESULTS AND DISCUSSION | 24 |
| 7 | CONCLUSIONS | 29 |
| | REFERENCES | 31 |
| | AUTHOR'S PUBLICATIONS | 38 |
| | CURRICULUM VITAE | 40 |
| | ABSTRACT | 42 |

1 INTRODUCTION

Railway transportation network has high demands in terms of energy savings, reliability and safety. The movement of people and goods between cities, as well as city public transportation is highly represented by the railway sector. This is the result of the continuing pressure for environmentally friendly and sustainable transportation. Furthermore, the growing popularity of high-speed trains gives rise to new advances in the field of railway research and development.

A key role in the operation of railway vehicle is the contact area between the wheel and rail where traction and braking forces are transferred. Contact mechanics affect not only the acceleration and deceleration of the vehicle, but also the dynamic behaviour. The dynamics greatly influence passenger comfort, running safety and service life. Issues such as derailment, high level of noise and wheel-rail failure can be traced back to the contact interface between wheel and rail. The most important property of wheel-rail contact is friction, also referred to as adhesion in the field of railway industry. In the simplest case, high friction causes excessive wear of the surfaces, while too low friction can lead to issues with traction and braking of the vehicle. In terms of dynamics, frictional forces can cause excitation of vibration in different machine parts and lead to passenger discomfort and machine part failure.

As a result of the contact being an open system with a wide range of external influences, it is not feasible to control the friction in a simple manner. In past, the most common problem was low adhesion caused by environmental causes such as fallen leaves, rain or snow. The application of an abrasive material such as sand helps with adhesion forces as well as removing the contamination layer from surfaces. Nevertheless, hard particles promote surface damage and wear. Low adhesion is desirable in the contact between the wheel flange and the rail gauge. To reduce wear and geometrical changes in this high sliding area, grease lubrication systems are widely used. In recent decades, top of rail lubrication management, which aims to provide optimal frictional conditions in wheel-rail contact, has been gaining popularity. Top of rail products applied into wheel-rail contact increase fuel efficiency, reduce maintenance cost and mitigate noise emission. Understanding the possible risks of using these products and defining their proper use could bring benefits in increasing the effectiveness of railway transportation, as well as ensuring safety and comfort of not only passengers, but also people and residents in areas that use the railway network.

The aim of this doctoral thesis is to clarify the frictional properties of top of rail products using experimental and numerical methods. Special attention is paid to the causes of low adhesion issues when applying these materials, which could cause problems with traction and braking.

2 STATE OF THE ART

Since the first deployment of railway transportation, the wheels and rails have undergone a substantial evolution. Nevertheless, the main principles remained the same. In the present day, the running surface of the wheel has a conical shape and slowly changes its geometry to a wheel flange at the inner side that prevents the wheels from derailing. Generally, during a rolling of two bodies, there are four main dimensions that define the contact geometry. The rolling radius of the wheel is r_{1x} and the radius of lateral profile is r_{1y} . For the rail, the radius in the direction of rolling is r_{2x} , which for a straight rail is equal to infinity, and in the lateral direction r_{2y} . The first index defines the body it refers to and the second index defines the direction as shown by the Cartesian system in Fig. 2.1. The wheel rotates with an angular velocity ω_1 resulting in velocity of the vehicle v_1 . The velocity of the moving surface of wheel is \dot{x}_1 and if we take the ground as a reference, then the stationary rail has a surface velocity \dot{x}_2 equal to zero. The wheel is loaded by a normal force F_N resulting in a contact area with semi-axes a and b in the x and y direction, respectively. The resulting forces in x , y and z direction are longitudinal, lateral and normal respectively. The longitudinal forces are also referred to as tangential or creep forces.

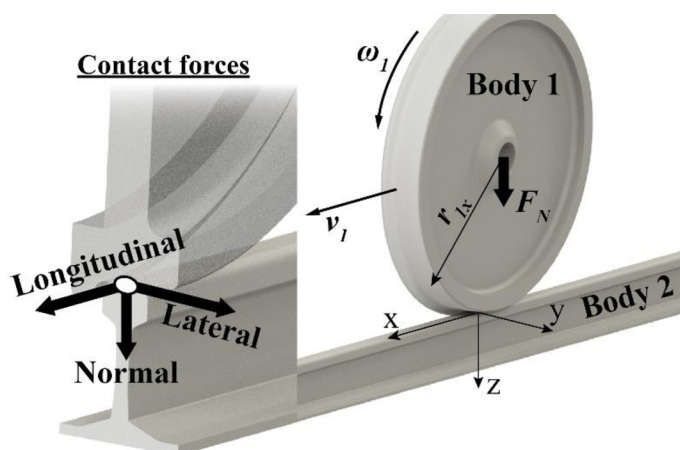


Fig. 2.1 Wheel-rail geometry and kinematics

Slip is defined based on the velocity of the vehicle and the vehicle wheel surface speed. SRR is defined based on the surface velocities divided by their mean value. In both cases, the number that is being divided represents the relative velocity between the two surfaces. Plotting the coefficient of adhesion versus slip gives a traction curve, as illustrated in Fig. 2.2. Looking closely, the contact area is divided to adhesion and microslip areas. At zero slip the bodies are in pure rolling conditions where no microslip conditions occur. With increasing slip between the two bodies, the coefficient of adhesion increases as area of slip also increases. At some point, the area of adhesion vanishes, and the contact is transferring tangential forces through full slip area. At this point, the coefficient of adhesion reaches the theoretical value of coefficient of friction, which is defined for full sliding conditions.

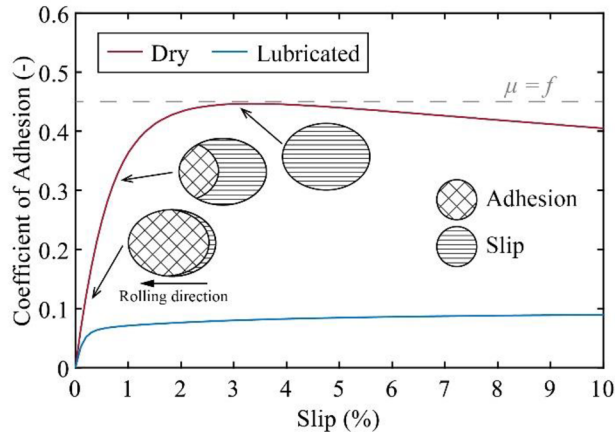


Fig. 2.2 Traction curve for dry and lubricated wheel-rail contact.

In Fig. 2.2 the traction curves for dry and lubricated contact conditions represent a real behaviour. With a higher slip, the coefficient of adhesion decreases for dry conditions. This is called a negative trend of the traction curve and is a result of increased temperature. For lubricated contact conditions, the traction curve reaches stable values, resulting in a negative or positive trend. The trend of the traction curve is important for the dynamic behaviour and stick-slip oscillations that occur under negative traction conditions.

In the presence of lubricant, the coefficient of adhesion is lower compared to clean and dry contact. Lubrication can be done with either solid or liquid lubricant. In the case of solid lubricant, the slip is accommodated by a layer of solid lubricant that has low shear strength. For liquid lubrication, we must consider the hydrodynamic effect that creates surface separation, as well as lubricant viscosity. This is best illustrated by the Stribeck curve in sFig. 2.3. The film parameter Λ describes the ratio between surface separation and surface roughness. At very low film parameters, the shear stresses are transferred mostly through asperity contacts. This is called a boundary regime, and the lubricant itself can have properties that create a very thin molecular film that help lower the coefficient of adhesion. With an increasing film parameter, the shear stresses are taken partly by asperity contact and partly by the lubricant film

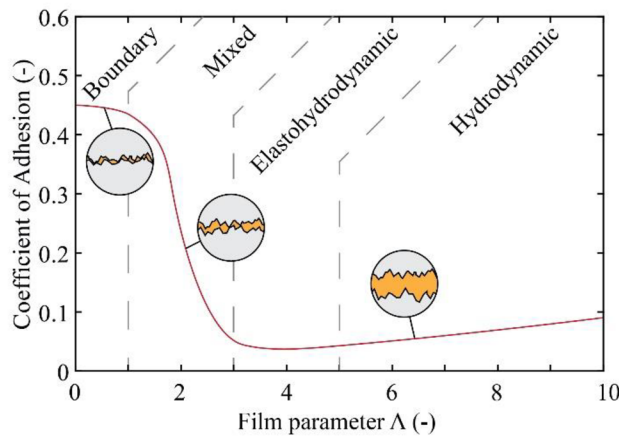


Fig. 2.3 Illustration of Stribeck curve.

in mixed lubrication regime. Going higher with film parameter transitions to the elastohydrodynamic regime, and the hydrodynamic regime where full separation of surfaces is achieved. At this point, friction is driven by the shear stress in the lubricant film, which is related to the viscosity of the lubricant.

2.1 TOP OF RAIL PRODUCTS

The general categorization of products used for wheel-rail contact friction modification is based on articles [3–5]. Friction management at the wheel-rail interface can be looked at in different ways. In the contact of the wheel flange and rail gauge, the use of low coefficient of friction (LCF) modifiers, such as greases, decreases wear. On the top of the rail, the increase in coefficient of adhesion by adhesion enhancers (very high positive friction modifiers – VHPF) is used in conditions that endanger traction and braking. In case of dry conditions when friction is too high for efficient operation, the use of top of rail management products is justified. These products are often classified as high positive friction (HPF) modifiers.

Managing the friction by HPF top of rail products leads to benefits in reduction of energy consumption, noise and damage to contacting surfaces such as wear, corrugation and rolling contact fatigue. Different types of products are applied to the contact interface for this purpose. We can differentiate these products based on the medium used to carry the components. Water-based substances are called friction modifiers (FM) and are meant to dry out after the substance is spread along the rail. Oil-based products are referred to as top of rail lubricants (TOR lubricant). In addition, products that use the benefits of both water and oil can be used (TOR hybrid). TOR hybrid products are often classified as TOR lubricants. Lastly, a solid material in the form of an interlocking blocks of sticks (solid FM) is available on the market. All these categories will be referred to as top of rail (TOR) products.

The effectiveness of TOR products has been reported in studies on vehicle dynamics [6–8], reduction of wear [9–15], corrugation [6, 16–20] and noise [21–24]. These studies might not be primarily focused on friction, which is the main aim of this thesis, and thus will not be described in further detail.

The purpose of the TOR product is to lower the coefficient of adhesion to a desirable level. A typical coefficient of adhesion for top of rail product is between 0.3 and 0.4 [3]. However, this can differ for field and laboratory experiments and is greatly influenced by the conditions of the surface and the used device. The study [25] compared the experimental results of various measuring devices for dry, wet and lubricated conditions. As seen in Fig. 2.4 for dry conditions, we get a wide range of measured coefficient of friction from 0.4 to 0.8. For friction modifier conditions, the data suggest more stable values around 0.15 – 0.25. For this reason, it is not easy to transfer the measured data between devices or even to real field conditions.

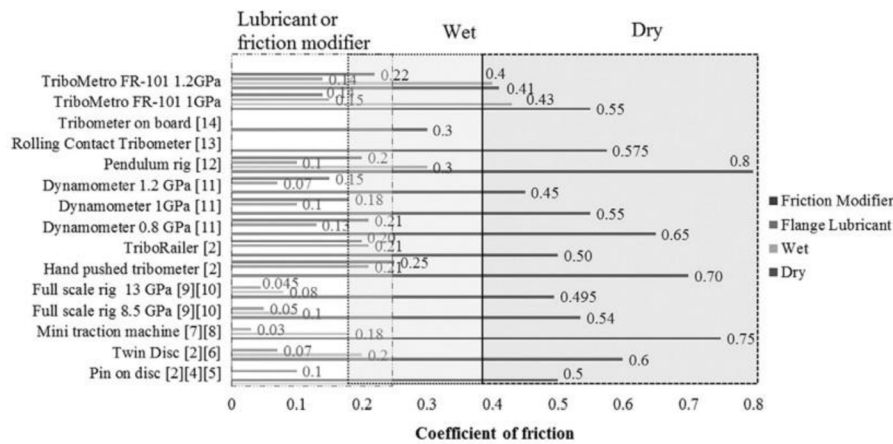


Fig. 2.4 Comparison of frictional values for different measuring devices and conditions [23].

The first study that brought to light the benefits of using friction management [26] used a solid FM product. However, the following studies to present day were mostly focused on water-based FM products and, in some cases, TOR lubricants/hybrid products. Only a handful of studies [35–37] used solid FM in experimental testing. Studies [35, 36] are also primarily focused on electric isolation that could be dangerous for the detection of trains. Interestingly, all the mentioned studies that used solid FM for frictional tests [26, 35–37] report a coefficient of friction of around 0.3 at higher slip ratio. For FMs, studies report coefficient of friction from 0.1 [25, 29, 40] up to 0.3 [22, 31], with the most occurring values being around 0.2 [11, 27, 29, 32]. TOR lubricants are not as thoroughly researched as FMs. Studies report values of around 0.1 [22, 34] up to 0.3 [12, 33]. However, the coefficient of adhesion for FM and TOR lubricant are dependent on the experimental device, methodology and application method. Normally, after application, the coefficient of adhesion drops to low values and slowly climbs to the optimal level where it should remain the longest time. After that, the film created from TOR product is removed and close to dry conditions are reached. When considering the dry FM film, the effect of initial drop is suppressed [11]. The TOR lubricant is more sensitive to applied amount and over-lubrication as suggested by studies [3, 12, 33, 34]. This is also true for TOR hybrid compositions [3, 34]. Taking into account studies dealing with VHPF and adhesion restoration [77, 78], it seems that the use of a higher hardness of particles or a higher amount of particles leads to faster recovery from low adhesion values after application.

The neutral to positive traction curve characteristic of TOR products is agreed upon by current studies. Intermediate levels of adhesion are experimentally confirmed under laboratory and field conditions. However, the application methodology plays a key role in the resulting coefficient of adhesion. Painting a TOR FM product with a brush caused low values of the coefficient of adhesion compared to spraying [29], where more stable values were achieved, as seen in Fig. 2.5. The spraying process provides a more spread and thinner layer, while brushing can leave an excessive amount of product on the surface. A decrease in coefficient of adhesion was also observed with high applied amounts of FM in HPT tests by Evans et al. [41]. Using

moderate amounts of non-commercial FM, Galas et al. [11] measured very stable intermediate levels of the coefficient of adhesion. With TOR lubricants and hybrid products, studies [10, 12, 33] showed a decreasing trend in the coefficient of adhesion with an increasing applied amount. Lower values were also seen in comparison with FMs in study by Hardwick [34]. This is reflected in review study by Stock. [3]. For solid FMs, the currently published papers focus primarily on traction curves with single application parameters. Direct comparison in coefficient of adhesion from published studies is not adequate due to different testing methodologies. Difficulty also being that the effect of applied amount is tied to the application method, experimental device, geometry of the specimen and contact area. Studies [10–12, 28, 33, 34] show that the coefficient of adhesion for TOR products is changing with running time of experiment. Based on selection of the time window for evaluation of the one point of traction curve, the results can vary considerably. On the other hand, using a continuous change in slip [29, 31] to measure the traction curve in one measurement run changes the interfacial layer by continuous removal of TOR product during the change of slip. This means that the state of contact interface constantly changes, and it is not valid to assume that same amount of TOR product is present at different slip conditions. This is supported by the study [29] in which subsequent tests without reapplication of FM resulted in a continuous increase in values of the traction curves.

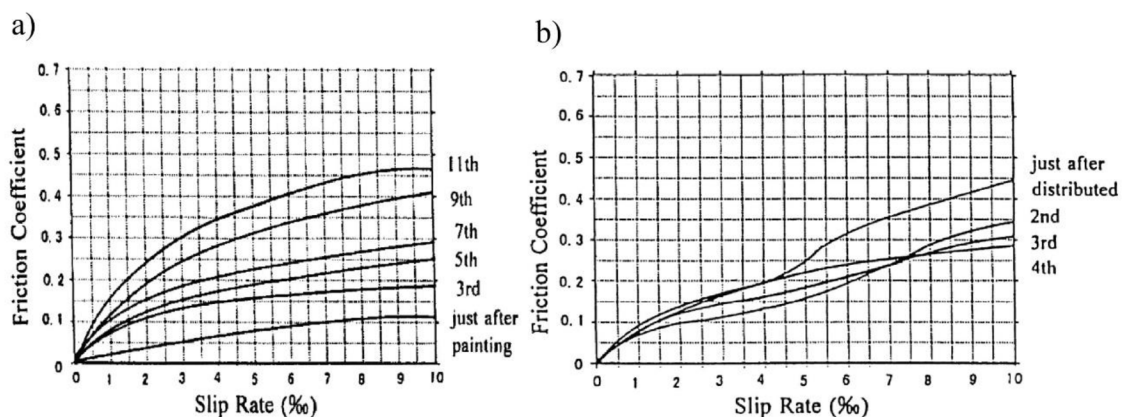


Fig. 2.5 Traction curves for painted HPF (a), sprayed HPF (b) [29].

Studies that focus on rheological properties provide shear stress-displacement characteristics for interfacial layers. This characteristic is key for modelling, as it provides information about the response of the contact interface to deformation caused by rolling-sliding motion. The first study [39] that introduced an approach based on the shear stress-displacement demonstrates a theoretical basis for predicting friction in contact with an artificial interfacial layer. This study used a pin-on-disc rheometer to measure the elasto-plastic behaviour of common contaminants. The same device was also used for TOR products in [31, 40]. Results from Harrison [31] show that HPF FM results in a low coefficient of friction in the initial low displacement region. With further sliding, the coefficient of friction reaches around 0.35 where it stabilizes.

At high displacements the dry conditions started to decrease in coefficient of friction which was not observed for TOR products. The results by [40] suggest a low coefficient of friction for FM below 0.1. No evident increase is seen for higher displacements as reported by [31]. These low values of the coefficient of friction seem to be the result of applying an excessive amount of FM. This is seen in study [41] where overapplication of FM dropped coefficient of friction below 0.05. The lower amounts applied reached values around 0.2 to 0.3 and with an increase in applied amount, the coefficient of friction decreases, as shown in Fig. 2.6. In the more recent use of shear stress-displacement characteristic for modelling of wheel and rail contact [41, 43, 44], a parametrization by Voce's hardening model [64] was used. The use of high pressure torsion device has been recently employed [41–44] to assess the shear response of various contact conditions.

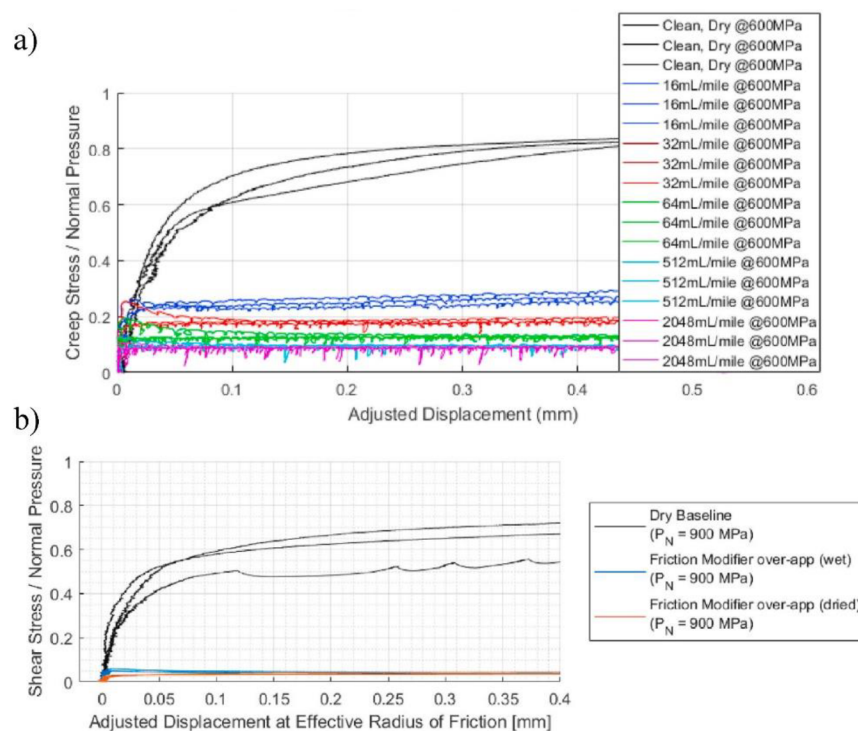


Fig. 2.6 Shear stress curves for applied amounts of TOR FM (a) and overapplication of TOR FM (b) [37].

Models for tangential contact forces need to be separated into two main areas: boundary and elastohydrodynamic friction. In the wheel and rail contact, studies mostly focus on expanding the boundary lubrication effects as the contact conditions point to the boundary regime. Experimental investigations showed that the original models [48, 50, 51, 53] do not predict the traction curve accurately. The two main deviations are in the initial slope of the traction curve and the decreasing trend at high slips. To resolve this, the original models were extended to accommodate for an accurate representation of experimental results. The modelling algorithm that is most built upon is Kalker's FASTSIM [48, 52, 53] that is used in studies [43, 44, 59, 61]. These studies show a good agreement between extended model predictions and

experimental data under various contact conditions and contamination. The main improvements come from using a variable coefficient of friction, either as a frictional function [59, 61] or by using material properties of the third body layer [43, 44]. In the study [62], the use of the material properties of third body layer in analytical model also yielded a good agreement with experimental data. The decrease in coefficient of adhesion is attributed to the increase in temperature. This is also taken into account in studies [43, 44, 56], where the estimation of contact temperature is shown in study [79].

As previously mentioned, FMs and TOR lubricants are based on liquid carrying medium. When modelling these materials, the effect of hydrodynamic lubrication should not be put aside. This was shown in the study [12] where excessively overlubricated contact with TOR lubricant behaved similarly to pure castor oil. It could also be the answer to very low adhesion conditions immediately after application of liquid TOR product, as seen in studies [10, 12, 33, 34]. Studies concerned with the elasto-hydrodynamic effect were mostly focused on water contaminated contact [65–69, 76]. The lubrication regime for wheel and rail contact can, in some cases, extend to mixed lubrication. In this case, the effect of roughness is important for accurate prediction of the coefficient of adhesion. The most commonly used models for asperity contact are statistical models of Greenwood and Williamson [70] and Greenwood and Tripp [72]. The study [73] used a newer model ZMC [74] that expands upon elasto-plastic deformations of asperities. However, the results were compared to Greenwood and Williamson model [70] with minimal differences for the selected conditions. The calculation of the coefficient of friction for mixed lubrication regime in these studies is based on the calculation of load portion carried by asperity and lubricant film. Both these portions have assigned coefficient of friction, which results in total coefficient of friction for the whole contact area. The coefficient of friction for lubricant film is mostly based on Newton's law of viscosity and the estimation of film thickness either by analytical formulas [65, 68] or using Reynold's equation [71, 73]. The coefficient of friction for asperity contact is assumed to be equivalent to friction in the boundary regime. However, studies [65, 68, 71] use a fixed coefficient of friction for asperity. The study [76] uses FASTSIM with varying coefficient of friction for asperity contact, allowing it calculation of different slips.

3 SUMMARY AND CONCLUSION OF STATE OF THE ART

The analysis of state of the art shows that a significant effort has been put into research of TOR products, mainly water-based FMs. Studies that use experimental methods to evaluate coefficient of adhesion for TOR products show that these products are able to reach optimal levels of adhesion and neutral to positive trend of traction curve that is linked with benefits such as better vehicle dynamics, fuel effectiveness, reduction of wear and noise. Nevertheless, the positive trend of the traction curve might not be a result of the product properties, but rather a reduction in the amount present in contact interface by means of increased slip. This results in non-steady-state conditions where the amount of TOR product in contact constantly changes. Using this information in a boundary model could explain the true shape of the traction curve under conditions of a set amount present in contact. In terms of low adhesion, the use of TOR lubricant is commonly associated with a low coefficient of adhesion, especially after application, as reported by studies [12, 22, 33, 34]. The exact causes for these low adhesion conditions are not yet fully explained. In terms of FM, the results diverge into studies reporting optimal adhesion levels [11, 27, 31], but also low levels [29, 32, 34] and in some cases even very close to dry conditions [22]. The use of different testing methodologies and applications results in inability to compare and deduce clear conclusions. However, it seems to be clear that FMs are much less sensitive to applied amount compared to TOR lubricants [3]. The drying process appears to be important [11], but has not yet been studied compared to different amounts and TOR lubricants. Such comparisons should be made on an experimental device using basic frictional principles to minimize the effect of application methodology and rolling-sliding contact. Lastly, solid FM was studied by only a handful of studies [26, 35, 37] that report very similar frictional values. However, the sensitivity of the applied product to the coefficient of adhesion was not yet examined.

Current frictional models that use elastohydrodynamics for wheel and rail contact focus mainly on water contamination [65–69, 76]. The limitation of these studies is the need for a boundary coefficient of friction that is based on estimation to fit experimental results [66, 68] or uses original boundary friction theories with a parametrized coefficient of friction [76]. Promising approach has recently been proposed, where purely boundary friction of various third body layers is represented by material properties of the contact interface [43, 44, 62]. The connection between boundary and elastohydrodynamic models is mostly done by means of statistical asperity models [70, 72, 74]. Nevertheless, a complete model using rheological properties for both the elastohydrodynamic and boundary regimes was not yet used and validated. Such model could use inputs from viscosity and surface shearing measurements to predict the coefficient of adhesion under various kinematic and loading conditions. This approach has also not yet been applied to the frictional properties of TOR products, where it could bring benefits in finding optimal use based on fundamental frictional properties.

4 AIM OF THESIS

The aim of this doctoral thesis is to use experimental and modelling methods to clarify the frictional behaviour of top of rail products. The main focus is to explain the causes of low adhesion conditions when using these products. The modelling approach will consider both boundary and elastohydrodynamic regime. As a result of the higher sensitivity to over-lubrication, a TOR lubricant will be used to assess the effect of composition and lubrication regime. Experimental methodology will be used to explain the characteristics of different types of TOR products currently available: FM, TOR lubricant and solid FM. The conditions leading to the risk of low adhesion will be evaluated. Subsequently, the model will be used to assess the traction curves of these products.

To achieve the main goal of this thesis, the solution of following sub-goals will be necessary:

- Frictional investigation of a TOR lubricants and use of model to assess the effect of boundary and elastohydrodynamic effects.
- Comparison of different TOR products by the application amount dependency on coefficient of friction.
- Development of a numerical model that considers both boundary and elastohydrodynamic lubrication regimes based on the rheological properties of the third body layer.
- Validation of the model using an experimental method with a model fluid.
- Assessment of causes leading to low adhesion conditions when using TOR products.
- The use of a model for the evaluation of steady-state traction curves of TOR products.

4.1 SCIENTIFIC QUESTION AND HYPOTHESES

Q1. How can the rheological properties be used with third body concept to predict the coefficient of adhesion in contaminated rolling-sliding contact?

H1.1 Knowing the shear response of solid-to-solid contact and lubricant viscosity can be used in Kalker's theory and general theory of elastohydrodynamics, combined with the asperity model to predict traction curves in contaminated rolling-sliding contact.

Q2. What is the cause of the low adhesion drop after application of the TOR lubricant and how can it be suppressed?

H2.1 Low adhesion after application of TOR lubricant is caused primarily by the hydrodynamic effect that shifts the contact to the mixed lubrication regime.

H2.2 Using large solid particles, which ensure asperity-particle-asperity interaction, will reduce initial drop and promote fast increase to optimal levels of adhesion after application of TOR lubricant.

Q3. What conditions pose a risk of low adhesion conditions for FM and solid FM?

- H3.1 The presence of liquid in FM will cause low adhesion, but after evaporation the undesirable conditions occur only when an excessive amount is applied.*
- H3.2 The composition of solid FM should provide a greater resilience to the applied amount compared to TOR lubricant.*
- Q4. What is the true shape of the traction curve under instantaneous contact conditions of the applied amount without the effects of time dependent TOR product removal?*
- H4.1 The use of TOR product does not result in a positive trend of traction curve as it only reduces the effects of temperature that causes a negative trend in dry contact.*

4.2 THESIS LAYOUT

This thesis is composed of three papers published in peer-reviewed journals. **Paper A** deals with the modelling approach of boundary and elasto-hydrodynamic friction. The model is compared with frictional measurements on the ball-on-disc tribometer. Film thickness measurements were conducted to validate the prediction of asperity contact. The traction curves for various speeds were measured and compared with the model prediction. **Paper B** aims to investigate the properties of a custom-made TOR lubricant. The effects of different components are examined, and rheological measurements were conducted for selected compositions to acquire inputs into the numerical model. The model is then used to evaluate the low adhesion conditions that occur immediately after application. The selected compositions were also compared with the commercial TOR lubricant. **Paper C** uses a high-pressure torsion device to assess the boundary lubrication properties of FM, TOR lubricant and solid FM. Different application amounts were used to understand the sensitivity of these products to the amount applied. The numerical model is extended with thermal effects, which were also measured by the experimental device. A wheel-rail contact model was used to assess the traction curves of different products.

Paper A

KVARDA, D., R. GALAS, M. OMASTA, L.B. SHI, H.H. DING, W.J. WANG, I. KRUPKA and M. HARTL. Asperity-based model for prediction of traction in water-contaminated wheel-rail contact. *Tribology International*, 2021, 157, 1–11.

Paper B

KVARDA, D., S. SKURKA, R. GALAS, M. OMASTA, L.B. SHI, H.H. DING, W.J. WANG, I. KRUPKA and M. HARTL. The effect of top of rail lubricant composition on adhesion and rheological behaviour. *Engineering Science and Technology, an International Journal*. 2022, 35, 1–9.

Paper C

KVARDA, D., R. GALAS, M. OMASTA, M. HARTL, I. KRUPKA and M. DZIMKO. Shear properties of top-of-rail products in numerical modelling. *Proceedings of the Institution of Mechanical Engineers, Part F: Journal of Rail and Rapid Transit*. 2022, 0, 1–10.

5 MATERIALS AND METHODS

5.1 LABORATORY MEASUREMENTS

5.1.1 Optical ball on disc tribometer

An optical tribometer was used to measure the coefficient of friction and film thickness between contact of a 25.4 mm diameter bearing steel ball and a BK7 glass disc. Both ball and disc are separately driven by servomotors allowing a precise control over rolling-sliding conditions. The disc is mounted with a lever arm that loads the disc against the ball and a force transducer is used for accurate measurement of normal load. A torque transducer is connected to the ball drive shaft for the measurement of coefficient of adhesion with a frequency of 1 kHz. The device uses a principle of colorimetric interferometry to measure the film thickness in the contact area. A light source enters the microscope, where it is directed into the lens that is focused into the contact area. The glass disc has a thin chromium coating that causes part of the light beam to reflect. The rest of the light beam enters into the contact and reflects from the surface of the ball. The part reflection from the chromium layer and part reflection from the ball surface cause an interference image that is recorded by the CCD camera and analysed by the software. The exact film thickness is calculated based on a calibration of static contact.

5.1.2 Mini traction machine ball on disc tribometer

The ball on disc tribometer is a commercial device Mini Traction Machine (MTM) produced by PCS Instruments Ltd in the United Kingdom. The device enables measurement of coefficient of adhesion between 19.05 mm diameter ball and 46 mm diameter disc. Alternative specimens and equipment are available, however, only the above-mentioned specimen dimensions were used. Both the ball and the disc are independently driven by a servomotor, enabling precise control over the rolling-sliding contact conditions. The driving mechanism of the ball is mounted on a lever arm, which enables the loading of the ball against the disc. The lever arm is equipped with a force transducer that measures the loading force. A second force transducer is used to measure the frictional force. The normal load can be set from 0 to 70 N, resulting in a 0 to 1.25 GPa maximum Hertzian contact pressure. The speed is controlled from -4 to 4 m/s and SRR from -200% to 200%. The software records all the parameters, as well as temperatures and wear rate with a frequency of 1 Hz.

5.1.3 Torsion rheometer

A high pressure torsion (HPT) rheometer is a device used for measuring rheological properties of interfacial layers. The device is designed by the author of this thesis and is based on devices used in studies [39, 42–44]. The construction of the device comes

from a friction and wear testing station R-MAT 3, originally developed at Brno University of Technology. The device uses a lower specimen with a flat surface and an upper specimen with an annulus with outer diameter of 12 mm and inner diameter of 6 mm. This results in a contact area of 85 mm². The lower specimen is held in a specimen holder that is fixed to a loading platform that can move up and down. The loading platform is loaded with hydraulic cylinder, resulting in a maximum loading force of 100 kN. The loading platform is made of a metal plate with high stiffness in the torsional loading direction, but is able to slightly bend in the normal direction. An alignment washer is used between the hydraulic cylinder and the loading platform to allow a slight correction of parallelism between the upper and lower specimen. The upper specimen is held in a specimen holder that is fixed to a shaft with a loading arm. The loading arm uses a screw jack to rotate the upper specimen. Between the screw jack and the loading arm is a force transducer that measures the force exerted on the arm, which is recalculated to torque. The maximum torque allowed is 400 Nm. The shaft is equipped with a rotary encoder that is used to calculate the displacement at the effective radius of the contact specimen. In addition, the rotational position of the worm screw driving motor is used to obtain a more accurate angle of the loading arm. The arm angle resolution is 0.00045 degrees, which corresponds to around 20 nm of displacement at the effective radius. Additionally, a heating segment can be attached with cartridge heating elements. This allows measurements at increased temperatures up to 100 °C.

5.2 NUMERICAL MODEL

The numerical model consists of three main routines. The first routine calculates the parameters of elastohydrodynamic friction. Second routine calculates boundary friction parameters. The third routine connects both elastohydrodynamic and boundary solution with asperity contact model. The calculation scheme that explains the algorithm is shown in Fig. 5.1.

The calculation of normal contact follows the Hertzian contact theory [80]. Approximate solution described in [81,82] is used. The origin of coordinate system is placed in the centre of contact area. At this point the contact pressure reaches maximum value.

The calculation of boundary coefficient of friction is based on the FASTSIM [48,52,53] algorithm. An extension is made by assuming third body layer in a similar way as described in [43,44] and frictional heating. A full theory analysis and equation derivation will not be given as it can be found in [48,52,53]. Only a simple longitudinal rolling is assumed.

In the simplified theory used by FASTSIM algorithm [48,52,53] it is assumed that the surface displacements and arising shear stresses have linear relationship. The linearity is given by Kalker's coefficients of flexibility. These coefficients are also determined for longitudinal, lateral and spin. As this thesis only deals with longitudinal direction, only the coefficient of flexibility in longitudinal direction is assumed.

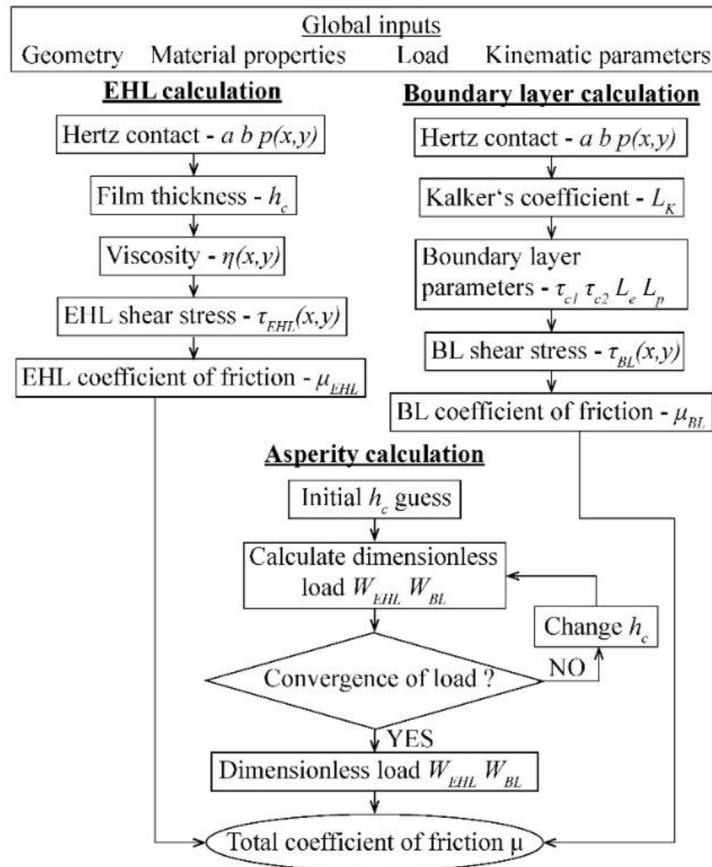


Fig. 5.1 Calculation scheme of numerical model.

Here we introduce the concept of third body layer. An elasto-plastic behaviour using Voce's hardening law [64], as shown in Fig. 5.2, is considered. The third body layer is characterized by limiting shear stress of elastic deformation τ_e , limiting shear stress of plastic deformation τ_p , elasticity parameter L_e and plasticity parameter L_p . As explained by [43,44,61], the resulting coefficient of flexibility in elastic part is given by sum of each individual coefficient of flexibility.

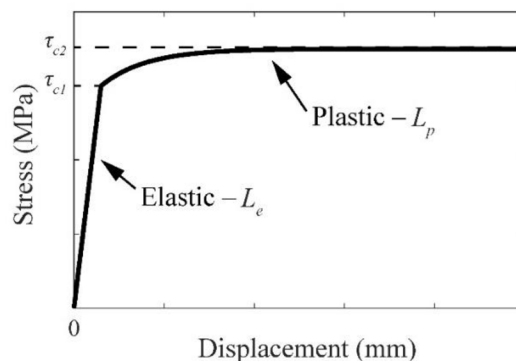


Fig. 5.2 Hardening material model.

Using the calculation described by FASTSIM algorithm we solve equation for shear stress. These equations use the assumption of elasto-plastic material behaviour. To solve this equation, a discretization of contact area is done. The contact area is divided

into n number of longitudinal strips with Δy width. Each strip is then divided into m number of points with distance of Δx . The algorithm runs through each strip where the solution in each point is acquired.

The calculation of elastohydrodynamic friction uses a Newton's law of viscosity. A critical parameter is the separation of surfaces, which is also referred to as film thickness. The calculation of film thickness can be done by using one of many approaches. However, in this model an analytical formula is used. It provides good enough accuracy with the benefit of much faster calculation time. Two equations are used here, one for iso-viscous regime and second one for piezo-viscous regime. In the iso-viscous regime, no change of viscosity with pressure is assumed. This is relevant for simple models of water, where change of viscosity with pressure is much smaller compared to oil. For iso-viscous regime the formula for central film thickness by Esfahanian and Hamrock [83] is used. For piezo viscous regime the formula of Hamrock and Dowson [84] is used.

To calculate the shear stress in the lubricant film, the same discretization, as was described for boundary friction, is used. In each point the shear stress is calculated.

The viscosity in each point is calculated using Roelands pressure-viscosity dependency [85]. However, if iso-viscous regime is considered than viscosity at each point is equal to viscosity at ambient conditions. The Barus equation is more simple formula which is used to experimentally find the pressure-viscosity coefficient. The resulting coefficient of friction in elastohydrodynamic regime is defined as shear stress divided by normal stress.

Now that the calculation of friction in both boundary and elastohydrodynamic regime is defined, a model for mixed lubrication regime will be explained. The calculation is based on theory of Greenwood and Tripp [72], that estimates the pressure carried by asperity interaction. The theory assumes paraboloidal asperities with Gaussian height distribution. The parameters that define these asperities are height standard deviation, curvature of asperity peak and density of asperity peaks. Two models of asperity deformation are used: elastic and plastic.

The calculation process starts with initial guess of film thickness that is taken from prediction formula. This initial guess assumes that all load is carried by lubrication film. Then the mean asperity pressure is calculated based on the deformation regime (elastic, plastic) that is considered. Using the mean asperity pressure, the non-dimensional load carried by asperities is determined.

The terminating condition for the error calculation is set to 0.1%. If the first iteration does not meet this condition, a set change of surface separation is done. This provides first two point which are then taken by the Newton-Raphson numerical method. The calculation then continues until the convergence condition is met. At the end of the calculation, the non-dimensional load carried by asperity and non-dimensional load carried by lubrication film are known. Using these parameters, the coefficient of adhesion is calculated.

The temperature calculation is based on solution provided by Ertz and Knothe [79]. The frictional power dissipation rate is a result of shear stress and rigid slip in contact

patch. Firstly, the shear stresses are found, as described in previous sub-sections. Then the power dissipation rate and temperature distribution are calculated. The temperature distribution is then used again in a new calculation of shear stress where temperature dependent variables change. Since both shear stress and temperature are dependent on each other, an iterative process is needed to reach convergence. This convergence cycle is repeated until the change in temperature is smaller than 0.1 °C.

5.3 TEST SAMPLES, EXPERIMENTAL CONDITIONS AND EXPERIMENT DESIGN

5.3.1 Paper A

This paper deals with the description and validation of a numerical model for the prediction of friction in liquid-contaminated contact. The experimental validation is done using an optical ball on disc tribometer with the ability to measure film thickness by means of colorimetric interferometry. Water is used as a reference liquid. It was chosen mainly to provide a wider range of mixed lubrication in the measurement speed range. Due to the very low roughness of the contact specimen the film thickness needs to be very low and thus oils were not suitable.

A 25.4 mm diameter ball made of bearing steel AISI 52100 with 53HRC (standard deviation 0.3HRC) hardness was used. This corresponds to 6 GPa for parameter H . Two types of surface roughness conditions were used in this study. A smooth surface of the ball was prepared by polishing with a diamond paste. A rough surface was prepared by a run-in procedure with maximum Hertzian pressure 0.75 GPa, 5% SRR and 500 mm/s speed. The resulting parameters of the surface measured by the optical profilometer are stated in Tab. 5.1. The calculation uses only these parameters, as the roughness of the glass disc with chromium coating has roughness less than 1 nm. These procedures were selected as they provided the most stable roughness condition during the experiment. The surface conditions were measured and evaluated after each experiment to confirm negligible changes. Also, the length of each measurement was made as short as possible. This was done to eliminate the effect of wear as well as damage to chromium layer.

Tab. 5.1 Surface parameters of ball specimen

| Surface condition | Roughness standard deviation ψ (nm) | Asperity peak curvature β (mm) | Asperity peak density γ (1/mm ²) | K (-) |
|-------------------|--|--------------------------------------|---|--------|
| Smooth | 8.3 | 0.301 | 24 200 | 0.0605 |
| Rough | 9.56 | 0.373 | 21 500 | 0.0767 |

The water used as a lubricant was previously distilled to guarantee its pureness. It was applied using a needle placed 5 mm in front of the contact. The supply of water was continuous to provide fully flooded conditions. The viscosity of 1 mPa·s is taken from [88], based on the room temperature.

Three types of tests were conducted: traction tests, film thickness measurement and Stribeck test. All tests were carried out under maximum Hertzian pressure of 0.75 GPa. The first test measured the traction curve and was aimed at identifying the boundary layer parameters. As mentioned before, the temperature dependency was neglected in the calculation. The second test measured the film thickness under 0% SRR. These measurements were used to compare the accurate prediction of film thickness by the model, which is important for the calculation of mean asperity pressure. Stribeck tests were then measured for both surface conditions. These results of the rough and smooth surface were then compared with the coefficient of adhesion prediction by both elastic and plastic asperity model. Lastly, a traction test under 5 different speeds was conducted. Only a rough surface was used for this, as it resulted in a broader mixed lubrication regime. Values from negative to positive SRR were measured and transformed to positive values to confirm the symmetrical behaviour with respect to 0% SRR. Each measurement point of the coefficient of adhesion is an average from a 4 second long interval at set measurement conditions. All types of tests with experimental conditions are shown in Tab. 5.2.

Tab. 5.2 Experimental parameters for all types of tests.

| Test type | Roughness type | Speed (m/s) | SRR (%) |
|----------------|----------------|----------------------|----------|
| Dry traction | Rough | 0.5 | -10 – 10 |
| Film thickness | Smooth | 0 – 2 | 0 |
| Stribeck | Smooth | 0.1 – 2 | 5 |
| Stribeck | Rough | 0.1 – 2 | 5 |
| Traction | Rough | 0.25, 0.5, 1, 1.5, 2 | -5 – 5 |

5.3.2 Paper B

The second paper uses both experimental and numerical tools to assess the frictional properties of TOR lubricants. The numerical model was extended with piezo-viscous elastohydrodynamic behaviour. The properties of the lubricants were measured by high pressure viscosimeter and HPT device. Different TOR lubricant components and compositions were tested using a ball on disc MTM machine. Custom TOR lubricants used a synthetic ester oil with bentonite thickener as a base medium. It was selected due to its good biodegradability. Additional constituents were friction modifier particles and solid lubricant. The list of all used components is seen in Tab. 5.3. All components were weighed using laboratory balance and mixed with shaft mixer for at least two hours before each experiment to ensure homogeneity of the composition.

For comparison, two commercial TOR lubricants were used. These are referred to as TOR A and TOR B. Both are hydrophobic biodegradable high pressure resistance lubricants. They are designed to reduce wear and squeal noise in railway curves.

Adhesion tests were conducted using MTM device with a specimen from bearing steel AISI 52100 with Vickers macro-hardness of 800–920 HV (ball) and 720–780

HV (disc). Hardened bearing steel does not represent real wheel and rail material. However, for comparative tests of TOR lubricants in a laboratory environment, the hardened steel provides minimal changes in surface topography during the tests. This ensures similar contact conditions during testing, which is desirable for quantitative comparison of tested substances. The tests were done under 800 MPa maximum Hertzian pressure, 2% SRR and 1 m/s speed. The contact pressure is typical for light-

Tab. 5.3 List of TOR lubricant constituents

| Component | Name | Particle size (μm) | Mohs hardness (-) |
|-----------------------------|--|---------------------------------|-------------------|
| Base medium | Synthetic ester oil with bentonite thickener | - | - |
| Friction modifier particles | Aluminium oxide | 10, 44 (D99) | 9 |
| | Zinc oxide | 5 (D99) | 4.5 |
| | Copper(I) sulfide | ≈ 5 | 2.5 |
| Solid lubricant | Graphite | 7 (D90) | 1-2 |
| | Molybdenum disulfide | 4.2 (D50) | 1-2 |

rail system. The speed was set based on the analysis of the lubrication regime and the parameter lambda, which corresponds to about 60 km/h in the train. The speed is also limited by the centrifugal effect, which removes the lubricant from the surface of the disc. The SRR was set to represent realistic conditions of wheel and rail contact. Higher values of SRR could cause excessive wear, which is a negative effect on stable surface conditions for all experiments. The experiments with different components were stopped at 20 minutes after application. The evaluation of the average coefficient of adhesion was taken after initial drop recovery until the end of the test, as shown in Fig. 5.3.

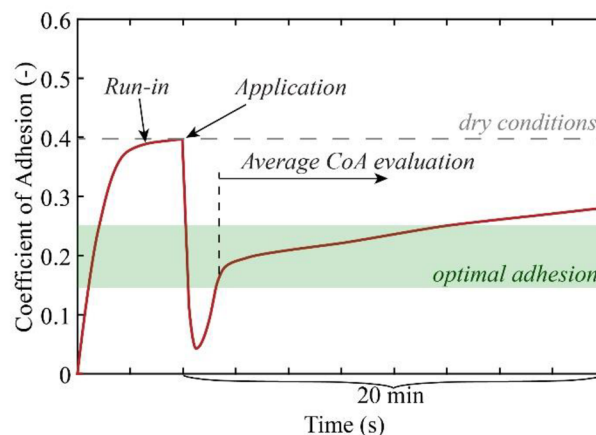


Fig. 5.3 Testing procedure for individual components of TOR lubricant.

Rheological tests were conducted using an HPT device to acquire boundary regime frictional properties. A high pressure viscosimeter was used for parameters of the base ester oil for the elastohydrodynamic part of the model. All HPT tests were done under 750 MPa normal pressure and displacement rate of 1 $\mu\text{m/s}$. The maximum shear displacement was set to 0.1 mm. The specimens used were made of DIN 100CrMn6 steel which has similar material properties to AIS 52100. The TOR lubricant was applied with a micropipette in 8 μl amount to ensure surface coverage. Before each HPT test a run-in was done. This run-in consisted of a 60 mm shear displacement at 500 MPa. The high pressure viscosimeter used only the base ester oil for tests. The viscosity was measured at 50 MPa steps up to 300 MPa at ambient temperature 25 $^{\circ}\text{C}$. The equations of Barus and Roelands were then used to estimate the pressure-viscosity coefficients.

5.3.3 Paper C

The last paper uses HPT device and boundary friction model to assess different types of TOR products and their performance. The tested TOR products are oil-based TOR lubricants (OFM 1 and OFM 2), water-based FM (WFM) and solid stick (SFM). Both OFM1 and OFM 2 use ester oil as a base medium. OFM1 uses organic thickener and is classified as NLGI 0. OFM2 uses inorganic thickener and has NLGI number 00. WFM contains water, thickener, solid lubricant and solid particles. SFM is made of a polymeric base with solid lubricant and solid particles for friction modification.

Since the experimental results use an HPT device, the numerical model neglects any effects of elastohydrodynamic lubrication. The boundary calculation is extended with temperature dependent parameters. The calculation parameters were selected based on a representative wheel and rail contact. Input parameters for the calculation are shown in Tab. 5.4. The input parameters of the boundary friction of the TOR products are part of the experimental results.

Tab. 5.4 Calculation parameters

| Parameter | Value | Unit |
|-------------------------------------|-------|-------------------|
| Longitudinal semi-axis a | 3.7 | mm |
| Lateral semi-axis b | 3.3 | mm |
| Rolling radius r | 350 | Mm |
| Normal force F | 20 | kN |
| Maximum Hertzian pressure p_0 | 790 | MPa |
| Thermal conductivity λ [87] | 50 | W/K·m |
| Density ρ | 7850 | kg/m ³ |
| Specific heat capacity c [87] | 450 | J/kg·K |

The contact specimens were made of DIN 100CrMn6 with 60HRC hardness. The material does not reflect the real material of the wheels and rails. However, this choice

was selected to provide more stable and comparable surface conditions for comparison of different TOR products. The selected material also reduces wear and suppresses any oxidation effects that could cause different conditions for experiments. The specimen surface was reconditioned for each tested product by polishing to remove any residue on the surface. The resulting surface roughness after polishing was $0.1 \mu\text{m}$.

The application of the tested liquid products was done using a micropipette. The applied liquid was spread along the contact patch to cover as much asperity contact as possible. In case of testing WFM at dry conditions, the applied product was dried by a heat gun set at $60 \text{ }^\circ\text{C}$. The solid stick was crushed into fine particles (particle size around $50 \mu\text{m}$) and the precise applied amount was weighed using laboratory balance. This does not correspond to the application methodology of these solid products. However, it allows the most precise control over the applied amount.

HPT tests were carried out under 750 MPa normal pressure which roughly corresponds to the maximum Hertzian contact pressure of light-rail system. The displacement rate was set to $1 \mu\text{m/s}$ with a maximum displacement of $400 \mu\text{m}$. The experiments under increased temperature used the same pressure and displacement rate. These tests were stopped after $200 \mu\text{m}$ displacement. Before each experiment, a run-in was conducted that was aimed at stabilizing the surface roughness around $0.3 \mu\text{m}$. This run-in phase also allowed to control the initial dry coefficient of friction that was around 0.5 at $400 \mu\text{m}$ displacement. Whenever surface roughness exceeded $0.4 \mu\text{m}$ after experiment the reconditioning process was repeated. After each experiment, the specimens were unloaded, cleaned with acetone in ultrasonic cleaner and surface roughness was measured. Resulting coefficient of friction data points are taken from an average value of last $20 \mu\text{m}$ of displacement before reaching maximum displacement, as shown in Fig. 5.4.

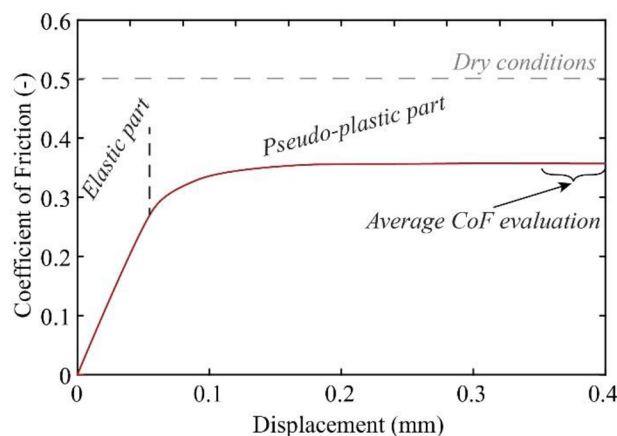


Fig. 5.4 HPT test illustration.

6 RESULTS AND DISCUSSION

This thesis aims to clarify the frictional characteristics of TOR products, especially focused on problems with low adhesion conditions. In the first part, a numerical model that calculates both boundary and elastohydrodynamic friction based on the third body model approach was proposed. Subsequently, this model was used to investigate the low adhesion conditions of TOR lubricants. Furthermore, the effect of different components of TOR lubricants was experimentally studied. Lastly, the boundary friction model is used together with experimental rheological measurements to assess the effect of amount of TOR products on coefficient of friction and low adhesion. The modelling approach helps identify the resulting traction curve characteristics. The findings can help with design of TOR products and defining strategy of their use and application.

The first step was to develop a numerical model that would use rheological inputs to predict coefficient of adhesion in contaminated rolling-sliding contact. **Paper A** presents a model for prediction of adhesion across the boundary, mixed and elastohydrodynamic regime. The model calculates the coefficient of adhesion based on the resulting shear stresses in the asperity contact and the lubricating film. The fact that the resulting friction is based on the rheological properties of the interface as a shear response to displacement (boundary regime) and rate of displacement (hydrodynamic regime) frees the solution from fixed values of the coefficient of friction.

The numerical model uses Kalker's FASTSIM algorithm to calculate surface displacements and resulting shear stresses based on third body layer rheology. This was previously proposed by Six et al. [43, 44] and similar approaches that use the parametrization of coefficient of friction proved to be applicable in various conditions [59, 61]. The elastohydrodynamic part uses the general law of viscosity to calculate shear stress in the lubricant film. Studies showed good agreement of this theory with experimental results [65, 66, 68, 73]. However, these studies also show that setting the correct coefficient of friction for the asperity contact is the key to obtaining relevant results. A workaround for these studies is to set this value in such a way that it corresponds to the experimental data. This is where the novelty of this study uses the results of improved FASTSIM to provide an accurate estimation of the boundary coefficient of friction in a simple calculation scheme. In this way, the calculation of shear stresses needs the rheological properties of the contact interface. The different running conditions can then be studied without knowing the coefficient of friction for each condition. The relative simplicity of the algorithm also allows for easy implementations of ideas such as lubricant shear thinning, temperature dependent parameters and different asperity models.

Initial experimental results using an optical tribometer under dry contact were used to identify boundary friction parameters. Saturated values of the coefficient of adhesion were relatively low, which was caused by the steel-glass configuration. During the main Stribeck and traction experiments, the film thickness measurement was only used to verify that no contamination occurred, and the film thickness is in a

correct range. If contamination occurred, the film thickness would rapidly increase above expected values, and the experiment needed to be redone. This approach helped control the contact conditions to ensure that parameters of the model prediction were correct.

The film thickness measurements verified a good accuracy of the analytical film prediction formula. The first Stribeck test with a smooth surface resulted in a very low coefficient of adhesion values across the measured speed range. Such a low coefficient of adhesion is a result of very low viscosity of water and very smooth surfaces. Similar values were observed in both the experimental and numerical works of Chen et al. [66, 68]. Under such a smooth surface as was used in this study, even a small surface separation enables the lubricating film to carry a large portion of the normal load. This is closely related to a modern topic in study of elastohydrodynamic superlubricity with low viscosity lubricants. The prediction using elastic asperity deformation heavily underestimates the coefficient of adhesion at low speed, but gets more accurate with higher speed. The lower load carried by asperity using the elastic deformation model was also shown in the original study by Greenwood and Tripp [72]. The results of asperity models showed that the estimation of the load carried by the lubricant film is a complex problem that is not easily solved by formulas using general simplifications. A future direction in using state of the art models could improve the accuracy across various experimental conditions as presented in studies [73, 75].

The proposed model showed a new way to incorporate the extended FASTSIM model and elastohydrodynamic theory to estimate the coefficient of adhesion in contaminated wheel-rail contact. The input rheological properties of dry contact and water implemented into FASTSIM and the general theory of elastohydrodynamic lubrication were able to accurately represent the experimental data with the correct use of the asperity model (**HYPOTHESIS H1.1 CONFIRMED**). However, the asperity model was valid for the used conditions and surface topography and does not have to be reasonably accurate for different surface topography. The use of the model is not limited to water contaminated contact, but by using a third body concept for boundary friction, it is suitable for various natural and artificial substances present in the contact interface. It should be noted that the asperity model is key to an accurate prediction of the mixed lubrication regime. The problematic of asperity contact needs to be thoroughly considered for different cases of contact conditions.

The tools described in **Paper A** were subsequently used together with experimental methods to answer the question regarding low adhesion conditions after the application of TOR lubricant in **Paper B**. The aim was to evaluate the low adhesion conditions of TOR lubricant composition while proposing a composition that reaches optimal levels of adhesion between 0.15–0.25 and is resilient to low coefficient of adhesion after application.

The initial experiments aimed to investigate the influence of individual components and their different contents in TOR lubricant. Experiments with solid lubricants were in line with a previous study [11] on the same device. It was found that use of solid particles for friction modification of medium hardness does not directly result in

higher frictional values in base medium. These results are in agreement with studies using zinc oxide in FM [11] and in water [78]. However, using a higher amount of medium hardness particles compared to high hardness aluminium oxide helped with lowering the sensitivity to application amount in study [12]. In this study, increasing the amount of solid particles did not lead to significant suppression of the initial drop. The addition of solid lubricant to the composition did not result in a significant reduction of effective coefficient of adhesion. Similar behaviour was shown in [40], where adding grease to FM did not result in an additional decrease in the coefficient of friction. This means that correct selection of friction modifier particles is key for the resulting frictional behaviour. It was also found that the use of excessive amounts of solid lubricant makes the composition a viscous paste, which causes problems with application with no additional benefits of coefficient of adhesion reduction. This needs to be taken into account when designing the product to ensure proper application in field use.

Based on the previous results, several compositions were compared with two commercial TOR lubricants. At the lowest applied amounts, all tested substances showed an increasing trend in coefficient of adhesion. This is typically observed with TOR products as a result of a low amount applied or high slip as seen in studies [12, 28, 33, 34]. With the higher amount, the commercial products resulted in over-lubrication as was also seen in [12, 34]. The custom-made substances stabilized at the optimal levels of adhesion with a very slow increase in the coefficient of adhesion until end of the experiment. This shape of time test results seem to be the most advantageous in achieving the optimal levels of adhesion for longer time. Similar trends were observed in studies [10, 12, 33]. However, the products that these studies use are much more sensitive to the applied amount, especially in [12]. Since this study uses the same small-scale ball on disc device, the geometry itself might be important in the low adhesion conditions seen.

The rheology measurements with the HPT device showed that the commercial product causes a low coefficient of adhesion in the boundary regime. This was not true for custom-made substances where the coefficient of friction reached optimal levels. The increasing trends in low application amounts are thus a result of removal of TOR product and increase in asperity contact. This would explain the slow increases seen in rheology testing of TOR products in [31]. Knowing the exact amount of product in the contact interface could help explain the transient effects of the coefficient of adhesion. A redistribution model could be built on this idea to simulate how long the applied product can be effective. Based on the model results, the initial drop for custom made substances seemed to be a result of not enough particles in the contact. Only the action of crushing the particles in combination with contact starvation will promote the boundary lubrication regime where the optimal levels of adhesion are reached.

Important conclusions are that the use of the model can help predict the coefficient of adhesion in boundary and elastohydrodynamic regime. Low adhesion conditions were the result of the solid particles providing not enough interaction between the

surfaces (**HYPOTHESIS H2.1 CONFIRMED**). The commercial product was not able to provide optimal levels of adhesion even in the boundary regime. This means that if the product is not spread into thin film, a low adhesion conditions will occur. Increasing the amount of solid particles for friction modification did not lead to effective suppression of low adhesion drop (**HYPOTHESIS H2.2 FALSIFIED**). The application methodology and the focus on creating a thin film seems to be the key to provide the longest effect with minimal risk to traction or braking.

Based on the findings in **Paper B**, where the boundary lubrication was found to be an important parameter for assessing the coefficient of adhesion, the boundary properties of different TOR products were investigated in **Paper C**. The aim of this study was to evaluate the low frictional properties and the application amount dependence of different TOR products. The numerical model was then used to assess the resulting trend of the traction curves.

The experimental results with TOR products show similar behaviour to studies [40, 41] and low displacement results in [31]. The application of FM in a dry state caused low friction only at a higher applied amount as suggested by [40, 41]. However, no low frictional values were observed when water was present, even at high applied amounts. This contradicts the findings of the study [11]. Suggesting the hydrodynamic effect does not seem to be a realistic explanation, as ball on disc tests with water do not generate enough surface separation compared to the scale of asperities and particles contained in FM. The results with a high amount of dry FM in this and previous studies [40, 41] could be explained by the formation of a compacted thick film that separates the surfaces. On the other hand, when water is present, the movement of particles is not constricted, and upon loading surfaces against each other, the particles can disperse and squeeze out with the help of water. This results in a thin film that allows for asperity interaction with hard particles of FM. In practice, when FM is applied, the wet state helps spread FM on the rail and provides an intermediate level of coefficient of friction. The action of spreading the product creates a thin film that upon drying contains a small amount of FM that cannot result in low frictional values. The only possible case where such low friction can occur is when FM is applied by the stationary unit and the film dries locally before the wheels can spread it. This results in a high amount of FM on a short section of rail creating low adhesion before the action of the wheel can remove it.

When comparing the applied amounts, the approximate density of TOR lubricant and FM can be interpreted that microliter applied results in around one milligram of product in the contact. As a result, the same trends of application sensitivity were seen for all tested products. Assuming the same mass of the TOR product in the contact, the levels of friction will be the same for the TOR lubricant, FM and solid FM. The explanation for the higher sensitivity of the TOR lubricant compared to FM [3, 34] could be a result of the effect described in the previous paragraph. After application of FM, the wet state provides high frictional values, and after drying, the film is too thin to create a thick layer that would cause low friction conditions. Regarding solid FM, even though the same sensitivity as that of the TOR lubricant was seen, the

vehicle application methodology used is not likely to overdose the contact with solid FM. However, this area is still not fully explored, as no detailed study about the application parameters of solid FM was published.

The investigation into the influence of temperature showed that TOR products suppress the effect of a decrease in coefficient of friction at a higher temperature seen in dry contact in this and other studies [89, 90]. However, the increased temperature does not cause an increasing trend in coefficient of friction. Similarly, the frictional tests do not show a prominent increase in coefficient of friction with higher displacement, as was also observed in [40, 41]. Since there is no process that would cause a dominant continuous increase in coefficient of adhesion with increase in slip, the traction curves show a neutral trend. This means, that the reported positive trends of traction curve [27–30] are a result of removal of the applied TOR product. As the friction of TOR product is dependent on the applied amount [10, 12], the measured traction curves do not exhibit purely slip-dependent behaviour, but also the influence of TOR product film removal. This could be especially important with the use of traction curves in dynamic modelling. Assuming a clearly positive trend of traction curve will not represent the reality of contact interface in discrete time instances.

The main findings of the last publication show that the presence of water medium in FM will not cause low adhesion conditions (**HYPOTHESIS H3.1 FALSIFIED**). If such conditions occur, it might be the result of used methodology, especially the use of small point contacts can lead to particles avoiding the leading edge of contact. When the mixture dried, low friction was observed with excessive amounts. However, if used correctly, this does not seem to hold true for wheel and rail application. All tested substances resulted in transition to low frictional values at the same amount present in contact. This means that FM and solid FM are not more resilient to the applied amount present in contact (**HYPOTHESIS H3.2 FALSIFIED**). It would be correct to state that it is easier to form a thin film and remove FM and solid FM, thus overall decreasing the amount in contact interface. It was found that the clearly positive trend of the traction curve is not a property of the TOR product, but it seems to be a result of decreasing the amount present in contact by increasing the sliding at higher slip (**HYPOTHESIS H4.1 CONFIRMED**).

7 CONCLUSIONS

The present dissertation thesis deals with the use of both experimental and numerical methods for evaluation of frictional performance of TOR products. The use of TOR products for reduction of wear, noise and energy requirements has been extensively studied in the last two decades. The current state of research shows that these benefits are linked to a reduction in coefficient of adhesion and a neutral to positive frictional characteristic. A large part of the published research used water-based FM products and less focus was aimed at TOR lubricants and solid FMs. The general conclusion can be made that the use of TOR lubricant poses a higher risk of over-lubrication and low adhesion conditions. However, even in some cases of FM use, there are lower than optimal levels of adhesion. To study these problems, the use of prediction models has not yet been extensively used. The main goal was to use experimental investigation and a numerical model to assess conditions that lead to low adhesion conditions when applying TOR product.

The results of this thesis are divided into three papers. The first paper dealt with introduction of the numerical model and its application on a model case of water contaminated contact. The model consists of a boundary friction part using Kalker's FASTSIM algorithm and elastohydrodynamic part governed by general Newton's law of viscosity. A statistical asperity model was used to provide connection between these two regimes to mixed lubrication. It was revealed that the correct use of the asperity model is detrimental to accurate prediction. The results showed that the combination of mentioned boundary and elastohydrodynamic models is usable for studying various third body contamination. The second paper used a commercial ball on disc tribometer and developed a numerical model to investigate the influence of TOR lubricant components on the coefficient of adhesion. Experiments with different types of particles in an oil-based medium showed that the hard solid particles have a dominant effect on the resulting friction. However, an important finding was that immediately after application, the particles were unable to rapidly increase the coefficient of adhesion from critical low levels. Application of the numerical model revealed that the initial drop was closely related to the change of lubrication regime. Only after a slow recovery did the coefficient of adhesion reach the boundary regime where it stabilized. Compared to commercial TOR lubricants, the custom-made composition showed good resilience to low adhesion. The last paper tested the boundary friction properties of TOR lubricant, FM and solid FM. It was found, that independently of the used product, the drop in coefficient of friction occurred at the same weight amount applied. Interestingly, the application of FM without drying the substance resulted in a higher coefficient of friction even after application of an excessive amount. The liquid state of this substance probably allows the movement of solid particles that results in more asperity or hard particle interaction.

This thesis contains original research expanding on knowledge regarding friction management in wheel and rail contact. The results are confronted with currently published research. Further work should be focused on extending the model by time-dependent changes in the coefficient of adhesion. This would provide information

about the redistribution and time effectiveness of the applied product. The main contributions of this thesis can be summarized in the following points:

- Numerical model considering both the boundary and elastohydrodynamic lubrication regime that can predict the coefficient of adhesion based on simple rheological test inputs.
- The use of large particles with high hardness does not improve resilience to low adhesion conditions after the application of TOR product.
- Low frictional values occur at the same amount of product present in the contact, regardless of the type of product used.

REFERENCES

- [1] STOCK, R., L. STANLAKE, C. HARDWICK, M. YU, D. EADIE and R. LEWIS. Material concepts for top of rail friction management – Classification, characterisation and application. *Wear*. 2016, 366–367, 225–232.
- [2] HARMON, M. and R. LEWIS. Review of top of rail friction modifier tribology. *Tribology - Materials, Surfaces & Interfaces*. 2016, 5831, 1–13.
- [3] KALOUSEK, J. and E. MAGEL. Modifying and managing friction. *Railway Track and Structures*. 1997, 93(5), 5–6.
- [4] EGANA, J. I., J. VINOLAS and N. GIL-NEGRETE. Effect of liquid high positive friction (HPF) modifier on wheel-rail contact and rail corrugation. *Tribology International*. 2005, 38(8), 769–774.
- [5] MATSUMOTO, A., Y. SATO, H. OHNO, M. TOMEOKA, K. MATSUMOTO, T. OGINO, M. TANIMOTO, Y. OKA and M. OKANO. Improvement of bogie curving performance by using friction modifier to rail/wheel interface Verification by full-scale rolling stand test. *Wear*. 2005, 258(7–8), 1201–1208.
- [6] OLDKNOW, K. D., D. T. EADIE and R. STOCK. The influence of precipitation and friction control agents on forces at the wheel/rail interface in heavy haul railways. *Journal of Rail and Rapid Transit*. 2012, 227(1), 86–93.
- [7] EADIE, D. T., D. ELVIDGE, K. D. OLDKNOW, R. STOCK, P. POINTNER, J. KALOUSEK and P. KLAUSER. The effects of top of rail friction modifier on wear and rolling contact fatigue: Full-scale rail-wheel test rig evaluation, analysis and modelling. *Wear*. 2008, 265(9–10), 1222–1230.
- [8] SEO, J.-W., H.-K. JUN, S.-J. KWON and D.-H. LEE. Effect of Friction Modifier on Rolling Contact Fatigue and Wear of Wheel and Rail Materials. *Tribology Transactions*. 2016, 0(0), 1–12.
- [9] GALAS, R., D. KVARDA, M. OMASTA, I. KRUPKA and M. HARTL. The role of constituents contained in water-based friction modifiers for top-of-rail application. *Tribology International*. 2018, 117, 87–97.
- [10] GALAS, R., M. OMASTA, I. KRUPKA and M. HARTL. Laboratory investigation of ability of oil-based friction modifiers to control adhesion at wheel-rail interface. *Wear*. 2016, 368–369, 230–238.
- [11] STOCK, R., D. T. EADIE, D. ELVIDGE and K. D. OLDKNOW. Influencing rolling contact fatigue through top of rail friction modifier application - A full scale wheel-rail test rig study. *Wear*. 2011, 271(1–2), 134–142.
- [12] EADIE, D. T., K. D. OLDKNOW, L. MAGLALANG, T. MAKOWSKY, R. REIFF, P. SROBA and W. POWELL. Implementation of wayside Top of rail friction control on North American heavy haul freight railways. In:

- Proceedings of the seventh World Congress on Rail- way Research.* 2006, 2–11.
- [13] SPIRYAGIN, M., M. SAJJAD, D. NIELSEN, Y. Q. SUN, D. RAMAN and G. CHATTOPADHYAY. Research methodology for evaluation of top-of-rail friction management in Australian heavy haul networks. In: *Proceedings of the Institution of Mechanical Engineers, Part F: Journal of Rail and Rapid Transit.* 2014, 228(6), 631–641.
- [14] EADIE, D. T., M. SANTORO, K. D. OLDKNOW and Y. OKA. Field studies of the effect of friction modifiers on short pitch corrugation generation in curves. *Wear.* 2008, 265(9–10), 1212–1221.
- [15] EADIE, D. T. and M. SANTORO. Top-of-rail friction control for curve noise mitigation and corrugation rate reduction. *Journal of Sound and Vibration.* 2006, 293(3–5), 747–757.
- [16] VUONG, T. T., P. A. MEEHAN, D. T. EADIE, K. D. OLDKNOW, D. ELVIDGE, P. A. BELLETTE and W. J. DANIEL. Investigation of a transitional wear model for wear and wear-type rail corrugation prediction. *Wear.* 2011, 271(1–2), 287–298.
- [17] ISHIDA, M., M. AKAMA, K. KASHIWAYA and A. KAPOOR. The current status of theory and practice on rail integrity in Japanese railways-rolling contact fatigue and corrugations. *Fatigue and Fracture of Engineering Materials and Structures.* 2003, 26(10), 909–919.
- [18] GRASSIE, S. L. Rail corrugation: Advances in measurement, understanding and treatment. *Wear.* 2005, 258(7–8), 1224–1234.
- [19] EADIE, D. T., M. SANTORO and W. POWELL. Local control of noise and vibration with KELTRACK friction modifier and Protector trackside application: An integrated solution. *Journal of Sound and Vibration.* 2003, 267(3), 761–772.
- [20] LIU, X. and P. A. MEEHAN. Investigation of squeal noise under positive friction characteristics condition provided by friction modifiers. *Journal of Sound and Vibration.* 2016, 371, 393–405.
- [21] EADIE, D. T., M. SANTORO and J. KALOUSEK. Railway noise and the effect of top of rail liquid friction modifiers: Changes in sound and vibration spectral distributions in curves. *Wear.* 2005, 258(7–8), 1148–1155.
- [22] EADIE, D. T., J. KALOUSEK and K. CHIDDICK. The role of high positive friction (HPF) modifier in the control of short pitch corrugations and related phenomena. *Wear.* 2002, 253(1–2), 185–192.
- [23] AREIZA, Y. A., S. I. GARCÉS, J. F. SANTA, G. VARGAS and A. TORO. Field measurement of coefficient of friction in rails using a hand-pushed tribometer. *Tribology International.* 2014, 82, 274–279.

- [24] KALOUSEK, J. and K. L. JOHNSON. An Investigation of Short Pitch Wheel and Rail Corrugations on the Vancouver Mass Transit System. *Proceedings of the Institution of Mechanical Engineers, Part F: Journal of Rail and Rapid Transit*. 1992, 206(2), 127-135.
- [25] LEWIS, R., E. A. GALLARDO, J. COTTER and D. T. EADIE. The effect of friction modifiers on wheel/rail isolation. *Wear*. 2011, 271(1-2), 71-77.
- [26] HARDWICK, C., S. LEWIS and R. LEWIS. The effect of friction modifiers on wheel/rail isolation at low axle loads. *Proceedings of the Institution of Mechanical Engineers, Part F: Journal of Rail and Rapid Transit*. 2014, 228(7), 768-783.
- [27] SONG, J., L. SHI, H. DING, R. GALAS, M. OMASTA, W. WANG, J. GUO, Q. LIU and M. HARTL. Effects of solid friction modifier on friction and rolling contact fatigue damage of wheel-rail surfaces. *Friction*. 2021.
- [28] LU, X., J. COTTER and D. T. EADIE. Laboratory study of the tribological properties of friction modifier thin films for friction control at the wheel/rail interface. *Wear*. 2005, 259(7-12), 1262-1269.
- [29] TOMEOKA, M., N. KABE, M. TANIMOTO, E. MIYAUCHI and M. NAKATA. Friction control between wheel and rail by means of on-board lubrication. *Wear*. 2002, 253(1-2), 124-129.
- [30] HARRISON, H., T. MCCANNEY and J. COTTER. Recent developments in coefficient of friction measurements at the rail/wheel interface. *Wear*. 2002, 253(1-2), 114-123.
- [31] MATSUMOTO, A., Y. SATO, H. ONO, Y. WANG, M. YAMAMOTO, M. TANIMOTO and Y. OKA. Creep force characteristics between rail and wheel on scaled model. *Wear*. 2002, 253(1-2), 199-203.
- [32] LUNDBERG, J., M. RANTATALO, C. WANHAINEN and J. CASSELGREN. Measurements of friction coefficients between rails lubricated with a friction modifier and the wheels of an IORE locomotive during real working conditions. *Wear*. 2015, 324-325, 109-117.
- [33] HARDWICK, C., R. LEWIS and R. STOCK. The effects of friction management materials on rail with pre existing rcf surface damage. *Wear*. 2017, 384-385, 50-60.
- [34] GALAS, R., M. OMASTA, M. KLAPKA, S. KAEWUNRUEN, I. KRUPKA and M. HARTL. Case study: The influence of oil-based friction modifier quantity on tram braking distance and noise. *Tribology in Industry*. 2017, 39(2), 198-206.
- [35] SHI, L. B., C. WANG, H. H. DING, D. KVARDA, R. GALAS, M. OMASTA, W. J. WANG, Q. Y. LIU and M. HARTL. Laboratory investigation on the

- particle-size effects in railway sanding: Comparisons between standard sand and its micro fragments. *Tribology International*. 2020, 146, 1–12.
- [36] WANG, C., L. B. SHI, H. H. DING, W. J. WANG, R. GALAS, J. GUO, Q. Y. LIU, Z. R. ZHOU and M. OMASTA. Adhesion and damage characteristics of wheel/rail using different mineral particles as adhesion enhancers. *Wear*. 2021, 477, 1–12.
- [37] EVANS, M., W. A. SKIPPER, L. E. BUCKLEY-JOHNSTONE, A. MEIERHOFER, K. SIX and R. LEWIS. The development of a high pressure torsion test methodology for simulating wheel/rail contacts. *Tribology International*. 2021, 156, 1–13.
- [38] MATSUMOTO, K., Y. SUDA, T. IWASA, T. FUJII, M. TOMEOKA, M. TANIMOTO, Y. KISHIMOTO and T. NAKAI. A Method to Apply Friction Modifier in Railway System. In: *JSME International Journal Series C*. 2004, 47(2), 482-487.
- [39] HOU, K., J. KALOUSEK and E. MAGEL. Rheological model of solid layer in rolling contact. *Wear*. 1997, 211(1), 134–140.
- [40] SIX, K., A. MEIERHOFER, G. TRUMMER, C BERNSTEINER, C. MARTE, G. MÜLLER, B. LUBER, P. DIETMAIER and M. ROSENBERGER. Plasticity in wheel–rail contact and its implications on vehicle–track interaction. *Proceedings of the Institution of Mechanical Engineers, Part F: Journal of Rail and Rapid Transit*. 2017, 231(5), 558–569.
- [41] SIX, K., A. MEIERHOFER, G. MUULLER and P. DIETMAIER. Physical processes in wheel-rail contact and its implications on vehicle-track interaction. *Vehicle System Dynamics*. 2015, 53(5), 635–650.
- [42] VOCE, E. The Relationship between Stress and Strain for Homogeneous Deformation. *Journal of the Institute of Metals*. 1948, 74, 537–562.
- [43] BUCKLEY-JOHNSTONE, L. E., G. TRUMMER, P. VOLTR, A. MEIERHOFER, K. SIX, D.I. FLETCHER and R. LEWIS. Assessing the impact of small amounts of water and iron oxides on adhesion in the wheel/rail interface using High Pressure Torsion testing. *Tribology International*. 2019, 135, 55–64.
- [44] VERMEULEN, P. J. and K. L. JOHNSON. Contact of Nonspherical Elastic Bodies Transmitting Tangential Forces. *Journal of Applied Mechanics*. 1964, 31(2), 338–340.
- [45] POLACH, O. A Fast Wheel-Rail Forces Calculation Computer Code. *Vehicle System Dynamics*. 1999, 33, 728–739.
- [46] KALKER, J. J. A Fast Algorithm for the Simplified Theory of Rolling Contact. *Vehicle System Dynamics: International Journal of Vehicle Mechanics and Mobility*. 1982, 11(1), 1–13.

- [47] KALKER, J. J. *Three-Dimensional Elastic Bodies in Rolling Contact*. Netherlands: Springer, 1990. 334 p. ISBN 9789048140664.
- [48] KALKER, J. J. Simplified Theory of Rolling Contact. *Delft Progress Report*. 1973, 1, 1–10.
- [49] SPIRYAGIN, M., O. POLACH and C. COLE. Creep force modelling for rail traction vehicles based on the Fastsim algorithm. *Vehicle System Dynamics*. 2013, 51(11), 1765–1783.
- [50] ROVIRA, A., A. RODA, R. LEWIS and M. B. MARSHALL. Application of Fastsim with variable coefficient of friction using twin disc experimental measurements. *Wear*. 2012, 274–275, 109–126.
- [51] MEIERHOFER, A., C. HARDWICK, R. LEWIS, K. SIX and P. DIETMAIER. Third body layer-experimental results and a model describing its influence on the traction coefficient. *Wear*. 2013, 314, 148–154.
- [52] ERTZ, M. and F. BUCHER. Improved Creep Force Model for Wheel/Rail Contact Considering Roughness and Temperature. *Vehicle System Dynamics*. 2002, 37, 314–325.
- [53] ERTZ, M. and K. KNOTHE. A comparison of analytical and numerical methods for the calculation of temperatures in wheel/rail contact. *Wear*. 2002, 253(3–4), 498–508.
- [54] CHEN, H., M. ISHIDA, A. NAMURA, K. S. BAEK, T. NAKAHARA, B. LEBAN and M. PAU. Estimation of wheel/rail adhesion coefficient under wet condition with measured boundary friction coefficient and real contact area. *Wear*. 2011, 271(1–2), 32–39.
- [55] CHEN, H., T. BAN, M. ISHIDA and T. NAKAHARA. Adhesion between rail/wheel under water lubricated contact. *Wear*. 2002, 253(1–2), 75–81.
- [56] CHEN, H., A. NAMURA, M. ISHIDA and T. NAKAHARA. Influence of axle load on wheel/rail adhesion under wet conditions in consideration of running speed and surface roughness. *Wear*. 2016, 366–367, 303–309.
- [57] CHEN, H., T. BAN, M. ISHIDA and T. NAKAHARA. Experimental investigation of influential factors on adhesion between wheel and rail under wet conditions. *Wear*. 2008, 265(9–10), 1504–1511.
- [58] CHEN, H., A. YOSHIMURA and T. OHYAMA. Numerical analysis for the influence of water film on adhesion between rail and wheel. *Proceedings of the Institution of Mechanical Engineers, Part J: Journal of Engineering Tribology*. 1998, 212(5), 359–368.
- [59] TOMBERGER, C., P. DIETMAIER, W. SEXTRO and K. SIX. Friction in wheel-rail contact: A model comprising interfacial fluids, surface roughness and temperature. *Wear*. 2011, 271(1–2), 2–12.

- [60] GREENWOOD, J. A. and J. B. P. WILLIAMSON. Contact of nominally flat surfaces. *Proceedings of the Royal Society of London. Series A. Mathematical and Physical Sciences*. 1966, 295(1442), 300–319.
- [61] GREENWOOD, J. A. and J. H. TRIPP. The Contact of Two Nominally Flat Rough Surfaces. *Proceedings of the Institution of Mechanical Engineers*. 1970, 185(1), 625–633.
- [62] WU, B., Z. WEN, T. WU and X. JIN. Analysis on thermal effect on high-speed wheel/rail adhesion under interfacial contamination using a three-dimensional model with surface roughness. *Wear*. 2016, 366–367, 95–104.
- [63] ZHAO, Y., D. M. MAIETTA and L. CHANG. An Asperity Microcontact Model Incorporating the Transition From Elastic Deformation to Fully Plastic Flow. *Journal of Tribology*. 2000, 122(1), 86–93.
- [64] WU, B., Z. WEN, H. WANG and X. JIN. Numerical analysis on wheel/rail adhesion under mixed contamination of oil and water with surface roughness. *Wear*. 2014, 314(1–2), 140–147.
- [65] ISHIDA, M., T. BAN, K. IIDA, H. ISHIDA and F. AOKI. Effect of moderating friction of wheel/rail interface on vehicle/track dynamic behaviour. *Wear*. 2008, 265(9–10), 1497–1503.
- [66] GODET, M. The third-body approach: A mechanical view of wear. *Wear*. 1984, 100(1–3), 437–452.
- [67] MEYMAND, S. Z., A. KEYLIN and M. AHMADIAN. A survey of wheel-rail contact models for rail vehicles. *Vehicle System Dynamics*. 2016, 54(3), 386–428.
- [68] VOLLEBREGT, E. A. H., K. SIX and O. POLACH. Challenges and progress in the understanding and modelling of the wheel–rail creep forces. *Vehicle System Dynamics*. 2021, 59(7), 1026–1068.
- [69] HERTZ, H. Über die Berührung fester elastischer Körper und über die Härte. *Jorunal für reine und angewandte Mathematik*. 1882, 92, 157–171.
- [70] PIOTROWSKI, J. and H. CHOLLET. Wheel-rail contact models for vehicle system dynamics including multi-point contact. *Vehicle System Dynamics*. 2005, 43(6–7), 455–483.
- [71] KALKER, J. J. *On the rolling contact of two elastic bodies in the presence of dry friction*. Delft, 1967. PhD thesis. Delft University of Technology. Faculty of Electrical Engineering, Mathematics and Computer Science.
- [72] LOGSTON, C. F. and G. S. ITAMI. Locomotive Friction-Creep Studies. *Journal of Engineering for Industry*. 1980, 102(3), 275–281.

- [73] SHEN, Z. Y., J. K. HEDRICK and J. A. ELKINS. A Comparison of Alternative Creep Force Models for Rail Vehicle Dynamic Analysis. *Vehicle System Dynamics*. 1983, 12(1–3), 79–83.
- [74] POLACH, O. Creep forces in simulations of traction vehicles running on adhesion limit. *Wear*. 2005, 258(7–8), 992–1000.
- [75] LOGSTON, C. F. and G. S. ITAMI. Locomotive Friction-Creep Studies. *Journal of Engineering for Industry*. 1980, 102(3), 275–281.
- [76] MEIERHOFER, A. *A new Wheel-Rail Creep Force Model based on Elasto-Plastic Third Body Layers*. Graz, 2015. PhD thesis. Graz University of Technology, Institute of Applied Mechanics.
- [77] WU, B., T. WU and B. AN. Numerical investigation on the high-speed wheel/rail adhesion under the starved interfacial contaminations with surface roughness. *Lubrication Science*. 2020, 32(3), 93–107.

AUTHOR'S PUBLICATIONS

Publications related to the topic of this thesis

KVARDA, D., R. GALAS, M. OMASTA, L.B. SHI, H.H. DING, W.J. WANG, I. KRUPKA and M. HARTL. Asperity-based model for prediction of traction in water-contaminated wheel-rail contact. *Tribology International*, 2021, 157, 1–11.

KVARDA, D., S. SKURKA, R. GALAS, M. OMASTA, L.B. SHI, H.H. DING, W.J. WANG, I. KRUPKA and M. HARTL. The effect of top of rail lubricant composition on adhesion and rheological behaviour. *Engineering Science and Technology, an International Journal*. 2022, 35, 1–9.

KVARDA, D., R. GALAS, M. OMASTA, M. DZIMKO, I. KRUPKA and M. HARTL. Shear properties of top-of-rail products in numerical modelling. *Proceedings of the Institution of Mechanical Engineers, Part F: Journal of Rail and Rapid Transit*. 2022, 0, 1–10.

Other publications

GALAS, R., D. KVARDA, M. OMASTA, I. KRUPKA and M. HARTL. The role of constituents contained in water-based friction modifiers for top-of-rail application. *Tribology International*. 2018, 117, 87–97.

SHI, L.B., Q. LI, D. KVARDA, R. GALAS, M. OMASTA, W.J. WANG, J. GUO and Q.Y. LIU. Study on the wheel/rail adhesion restoration and damage evolution in the single application of alumina particles. *Wear*. 2019, 426-427, 1807–1819.

SHI, L.B., C. WANG, H.H. DING, D. KVARDA, R. GALAS, M. OMASTA, W.J. WANG, Q.Y. LIU and M. HARTL. Laboratory investigation on the particle-size effects in railway sanding: Comparisons between standard sand and its micro fragments. *Tribology International*. 2020, 146, 1–12.

REMESOVA, M., S. TKACHENKO, D. KVARDA, I. ROCNAKOVA, B. GOLLAS, M. MENELAOU, L. CELKO and J. KAISER. Effects of anodizing conditions and the addition of Al₂O₃/PTFE particles on the microstructure and the mechanical properties of porous anodic coatings on the AA1050 aluminium alloy. *Applied Surface Science*. 2020, 513, 1–10.

LI, Q., B.N. WU, H.H. DING, R. GALAS, D. KVARDA, Q.Y. LIU, Z.R. ZHOU, M. OMASTA and W.J. WANG. Numerical prediction on the effect of friction modifiers on adhesion behaviours in the wheel-rail starved EHL contact. *Tribology International*. 2022, 170, 1–11.

NAVRATIL, V., R. GALAS, M. KLAPKA, D. KVARDA, M. OMASTA, L.B. SHI, H.H. DING, W.J. WANG, I. KRUPKA and M. HARTL. Wheel squeal noise in rail transport: the effect of friction modifier composition. *Tribology in Industry*. 2022, 44, 361–373.

LI, Q., S.Y. ZHANG, B.N. WU, Q. LIN, H.H DING, R. GALAS, D. KVARDA, M. OMASTA, W.J. WANG and Z.F. Wen. Analysis on the effect of starved elastohydrodynamic lubrication on the adhesion behavior and fatigue index of wheel-rail contact. *Wear*. 2022, 510-511, 1–12.

CURRICULUM VITAE

Ing. Daniel Kvarda

Date and place of birth: 23/09/1991, Brno

Education

- **2017 – 2022** Doctoral study at Institute of Machine and Industrial Design, Faculty of Mechanical Engineering, Brno University of Technology. Topic of the dissertation thesis: *Experimental investigation and numerical modelling of top of rail products*.
- **2015 – 2017** Master study at Institute of Machine and Industrial Design, Faculty of Mechanical Engineering, Brno University of Technology. Topic of the diploma thesis: *Influence of friction modifiers composition on traction in wheel-rail contact*.
- **2012 – 2015** Bachelor study at Faculty of Mechanical Engineering, Brno University of Technology. Topic of the bachelor thesis: *Animation of cylindrical gears meshing*.
- **2007 – 2011** Secondary Industrial School a Higher Technical School Brno, Sokolská 1. Specialization: Computer graphics.

Awards

- 2017 – Industrial Enterprise Award - Awarded by Honeywell for Outstanding Diploma Thesis

Teaching activities – seminars:

- 3CD - CAD
- 1K – Engineering Drawing Fundamentals
- 2K – Engineering Drawing
- ZSY-A – Finite Element Method – ANSYS Classic
- ZAW – Finite Element Method – ANSYS Workbench
- ZBW – Finite Element Method – Advanced Analyses
- ZAP – Analytical Project

Participations in scientific projects

- 2020 – 2022: Squeal noise generation in the wheel-rail contact with modified friction (GA20-23482S)
- 2019 – 2021: Study on key technologies and application strategies for wheel-rail friction management in rail transport (LTACH19001)
- 2016 – 2020: RISEN - Railway Infrastructure System Engineering Network (H2020-MCSA-RISE)

Internships

- Southwest Jiaotong University / China / 31/03/2018 / 04/08/2018
- Railway Technical Research Institute / Japan / 25/07/2019 / 07/11/2019
- Virtual Vehicle Research GmbH / Austria / 01/10/2021 / 31/03/2022

Language skills

Czech, English

Scientific activities

- Tribology of wheel-rail contact
- Lubricant flow in elastohydrodynamic contact
- Mathematical modelling of rolling-sliding contact
- FEM simulation of statically and dynamically loaded machine parts

ABSTRACT

This dissertation thesis deals with experimental and numerical study of top of rail products. These products are used to reduce wear, noise and improve energy efficiency of wheel and rail contact. In the last two decades, extensive experimental research has been conducted on the use of top of rail products. However, very little research has focused on the fundamental mechanisms of these products, especially causes of low adhesion. Application of mathematical models to this field was also not yet examined. The aim of this thesis is to explain the frictional behaviour and low adhesion conditions of the top of rail products with the use of a mathematical model. The model assumes both friction arising from solid asperity interaction and separation by a fluid film. The validation of this model was carried out on an experimental tribometer with the ability to measure film thickness to validate the accurate prediction of surface separation. A commercial tribometer was used to investigate the influence of individual components in oil-based top of rail product on the coefficient of adhesion. A set of rheological tests in combination with the model showed that the solid particles had very little effect in increasing adhesion after application. Subsequently, different types of top of rail products were tested using a high pressure torsion device. The boundary friction of these substances was evaluated by the model. The positive frictional characteristics that these products should provide are found to be a result of sliding friction changing the composition of the interfacial layer. In addition, the low coefficient of friction due to overapplication occurred at the same amount applied for all tested substances. This thesis presents original research expanding on the knowledge of top of rail products.

ABSTRAKT

Tato disertační práce se zabývá experimentálním a numerickým studiem maziv pro temeno kolejnice. Tyto maziva se používají ke snížení opotřebení, hluku a zlepšení energetické účinnosti kontaktu kola a kolejnice. V posledních dvou desetiletích byl proveden rozsáhlý experimentální výzkum týkající se použití maziv pro temeno kolejnice. Avšak velmi málo výzkumu bylo zaměřeno na základní mechanismy těchto produktů, zejména na problémy s nízkou adhezí. Aplikace matematických modelů v této oblasti také nebyla dosud zkoumána. Cílem této práce je pomocí matematického modelu vysvětlit třecí chování a problémy s nízkou adhezí maziv pro temeno kolejnice. Model předpokládá jak tření vznikající interakcí nerovností pevných látek, tak separaci mazacím filmem. Validace tohoto modelu byla provedena na experimentálním tribometru se schopností měřit tloušťku filmu pro ověření přesné predikce separace povrchu. Komerční tribometr byl použit ke zkoumání vlivu jednotlivých složek v mazivu pro temeno kolejnice na bázi oleje. Sada reologických testů v kombinaci s modelem ukázala, že pevné částice měly velmi malý vliv na zvýšení adheze po aplikaci. Následně byly testovány různé typy maziv pro temeno kolejnice pomocí vysokotlakého torzního zařízení. Mezný režim tření těchto látek byl hodnocen představeným modelem. Bylo zjištěno, že pozitivní třecí vlastnosti, které by tyto produkty měly poskytovat, jsou výsledkem velké skluzové vzdálenosti, která

mění složení třecí vrstvy. Nízký koeficient tření v důsledku nadměrné aplikace se vyskytl při stejném aplikovaném množství u všech testovaných látek. Tato diplomová práce představuje původní výzkum rozšiřující znalosti o produktech pro temeno kolejnice.